Chapter 6
Bearing Strength

Abstract The bearing strength of FMLs is discussed with respect to the individual constituent phenomena. In particular the two main methods to experimentally obtain the bearing strength are discussed, addressing ply delamination buckling as an important phenomenon. The influence of the various characteristic specimen dimensions on the bearing strength is discussed, and theories are presented to predict the bearing strength of FMLs based on their constituent materials.

6.1 Introduction

The bearing strength is an important parameter for static strength evaluations of mechanically fastened joints. The load transfer from one sheet to another sheet through pin loading requires assessment of the strength of the pin–hole detail and evaluation of the related failure mechanisms.

Aside from the rivet or bolt failure mode, the sheet may fail in different modes. These failure modes are illustrated in Fig. 6.1. The type of failure mode that occurs often depends on the geometrical dimensions of the pin–hole joint, i.e. the diameter-to-width ratio (D/W) and the edge distance-to-diameter ratio (e/D). High values of the D/W ratio often result in net-section failure, whereas low values of e/D often result in shear-out failure.

This chapter primarily focuses on the bearing strength failure, Fig. 6.1c. Similar to the blunt notch strength, discussed in the previous chapter, the failure phenomena for bearing strength in FMLs differ from metallic or fibre reinforced polymer composite materials. Bearing failure is defined as the given amount of permanent deformation of the hole loaded by the pin. In metals, this deformation is primarily caused by the plastic deformation of the material, while for composite materials, this deformation may be the result of delamination buckling, fibre buckling, fibre splitting and other fracture mechanisms.

This chapter starts by describing the definition of bearing strength as it is considered for mechanical joining in FMLs. The failure phenomena reported in the literature will be described to provide a background for the evaluation methods for bearing strength in FMLs given thereafter.

R. Alderliesten, *Fatigue and Fracture of Fibre Metal Laminates*, Solid Mechanics and Its Applications 236, DOI 10.1007/978-3-319-56227-8_6

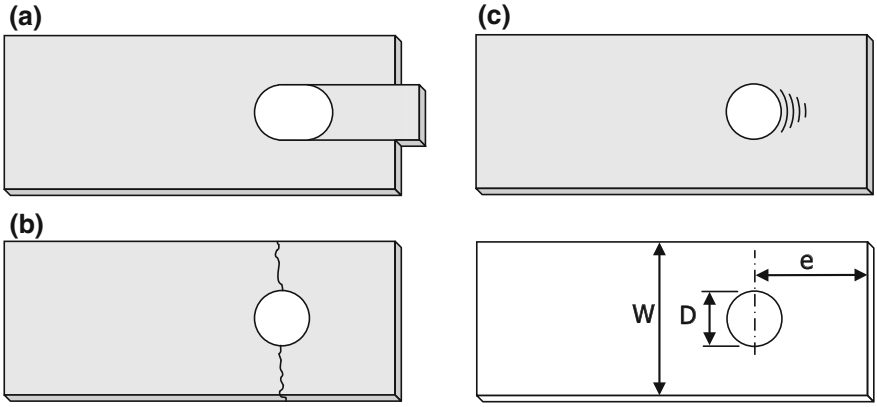

Fig. 6.1 Typical failure modes of pin-loaded holes; shear-out (**a**), net-section (**b**) and bearing failure (**c**)

6.2 Definition of Bearing Strength

The bearing strength is typically described as the pin load divided by the area defined by the pin diameter and sheet thickness, as illustrated in Fig. 6.2. The pin load required to cause failure is then referred to as the bearing ultimate strength (BUS).

Because the FMLs developed up until today have been certified as metallic structures, the bearing strength allowables are defined similar to the allowables for

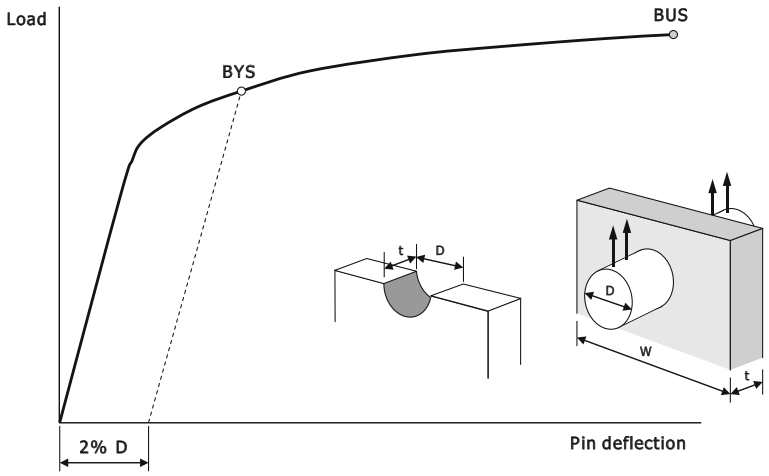

Fig. 6.2 Definition of the bearing allowables according to the ASTM standards [1]; the bearing strength is defined as the pin load divided by the area of pin diameter times thickness

monolithic metallic structures. These allowables are related to the bearing yield strength (BYS) and BUS illustrated in Fig. 6.2.

6.3 Failure Phenomena

6.3.1 Delamination Buckling

The failure modes that can occur during pin loading FMLs are either typical metallic or typical composite failure modes. The deformation indicated in Fig. 6.2 can be attributed to the plastic deformation of the metallic layers in the FML and to the composite fracture mechanisms at the same time. However, as a result of the laminated structure of FMLs, delamination buckling may occur as an additional failure mode when either the metallic layers are too thin, or when insufficient constraint is provided around the pin-loaded hole. The out-of-plane deformation of the laminate illustrated in Fig. 6.3 may induce interlaminar stresses of such magnitude that delamination between the layers occurs. This delamination implies that the layers are no longer joined and supported by each other, resulting in buckling of the individual metal layers.

As a consequence, the lack of hole constraint in the pin-bearing tests for metallic sheets [1] may be insufficient to observe bearing failure in the FML, making a pin-bearing test with anti-buckling constraints necessary [2]. This type of pin-bearing tests is often referred to as bolt bearing [3, 4], as it represents the clamping provided by the bolt head and washer. Typical BYS and BUS values for GLARE and ARALL laminates are given in Table 6.1.

The difference in typical load–deflection curves that one may obtain with either the ASTM E238-84 [1] or the ASTM D953-54 [2] test standard is illustrated in Fig. 6.4. Due to the lack of constraint in the first standard test, delamination buckling may occur at relatively low stress levels, whereas bearing failure modes can be observed when constraint is provided according to the latter standard test.

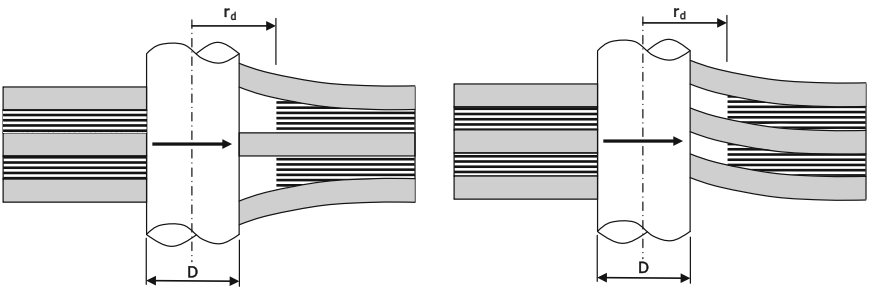

Fig. 6.3 Illustration of symmetric and asymmetric out-of-plane deformation due to pin loading [4]

Table 6.1 Standardized ARALL and GLARE grades [4]

Grade of laminate and lay-up	ASTM E238-84		ASTM D953-54	
	BYS[a] (MPa)	BUS[b] (MPa)	BYS (MPa)	BUS (MPa)
GLARE2-3/2-0.3	–	549	530	709
GLARE3-3/2-0.3	–	537	546	789
GLARE4-3/2-0.3	–	510	518	658
ARALL2-3/2-0.3	–	563	492	727
ARALL3-2/1-0.3	–	593	716	946
ARALL3-3/2-0.3	–	556	615	825

[a]Bearing yield strength could not be determined
[b]Failure by delamination buckling

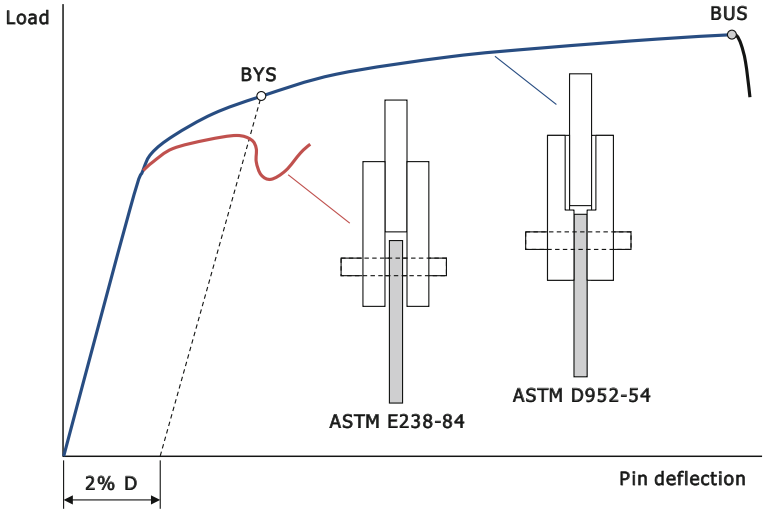

Fig. 6.4 Characteristics load–deflection curves for pin-bearing and bolt-bearing tests [4]

Slagter [4] investigated the strength of mechanically fastened joints in FMLs. He observed that in the numerous static failure tests performed on these types of joints, delamination buckling was not present. The constraint provided by the fastener head and joined sheets appears to be sufficient to prevent delamination buckling from occurring.

For assessment of the strength of mechanically fastened joints in FMLs, the bearing type of failure is therefore of prime interest. This means that for bearing strength, the characteristic load–deflection curve obtained with lateral constraint (ASTM D953-54 standard—illustrated in Fig. 6.4), is the curve of interest. Therefore, delamination buckling is not considered in the remainder of this chapter, and only bearing failure is discussed. More information on delamination buckling due to pin loading of holes is given by Slagter [4].

Another aspect often not explicitly addressed, but worth to note is the influence of the laminates Young's modulus on the determination of the BYS. This is illustrated for unidirectional and cross-play FMLs in Fig. 6.5. The offset definition of 2%D in the determination of BYS implicitly incorporates an influence of the elastic stiffness. In addition, depending of the amount of strain hardening after yielding FMLs with relatively higher BYSs may end up with relatively lower BUSs.

6.3.2 *Bearing Failure*

In experiments, the different failure modes illustrated in Fig. 6.1 may be chosen by carefully selecting the geometry of the specimens. Limiting the edge distance (e/D) too much will cause shear-out, while taking the diameter too large compared to the specimen width, most likely will give net-section failure.

However, although a standardized test may be defined for which the bearing type of failure mode is most common [7], the other failure modes may not be fully excluded. In fact, depending on the FML constituents considered, the specimen geometry may need to be redefined in order to avoid net-section failure or shear-out [8]. That fact even applies to the lateral constraint applied to the specimen [9]; depending on the thickness of the individual metallic sheets, even the slightest delamination may induce buckling of the metallic sheets.

In addition to that, the bearing failure mode may occur together with crack formation in width direction (initiation of net-section failure) and in loading direction (initiation of shear-out). This was observed by Buczynski [10] who tested

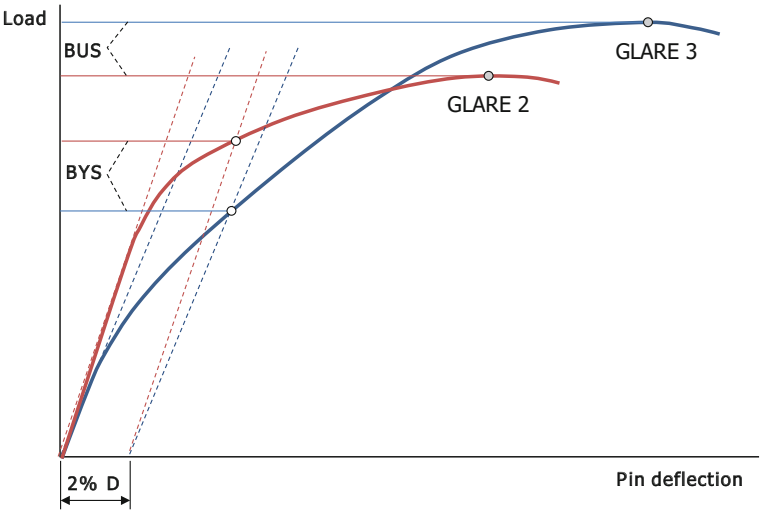

Fig. 6.5 Influence of Young's modulus on the measured BYS and BUS [5, 6]; note the similarity with the influence illustrated in Fig. 2.2

FMLs made of 0.1 mm thin stainless steel sheets reinforced by carbon fibre epoxy layers. The very thin sheets easily buckled due to the lack of lateral support, but the typical bearing failure often occurred together with shear-out cracking (Fig. 6.6) and net-section onset cracking (Fig. 6.7).

The observations of Buczynski are not exclusively related to the application of thin stainless steel foils, as demonstrated by the experimental observations of Frizzell et al. [11].

Here one should bear in mind that the definition of bearing strength, related to the 2%D deflection, may be easily obtained with, for example, ARALL and GLARE, containing ductile aluminium alloys, but requires more damage (mechanisms) before similar deflections or deformations are obtained with high stiffness stainless steel alloys and carbon fibre epoxy systems.

Cross sections made by Buczynski revealed a high amount of buckling deformation in the individual stainless steel sheets before 2% permanent deformation, see Fig. 6.8. The observations seem in agreement with the observations reported by

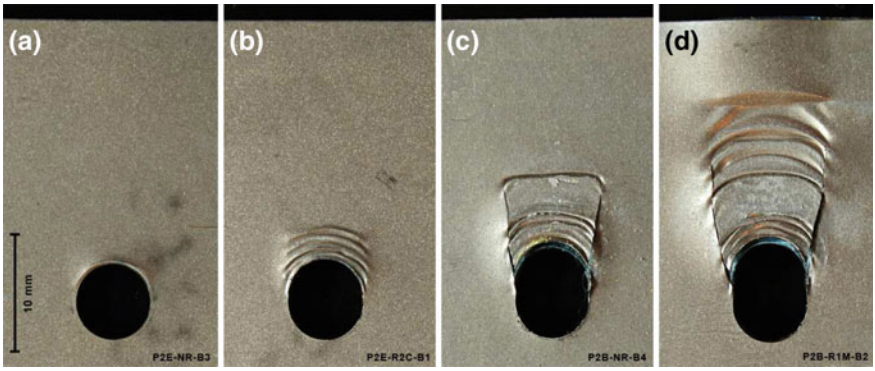

Fig. 6.6 Typical stages of bearing failure combined with buckling and shear-out cracking in stainless steel–CFRP laminates observed in four different specimens [10]

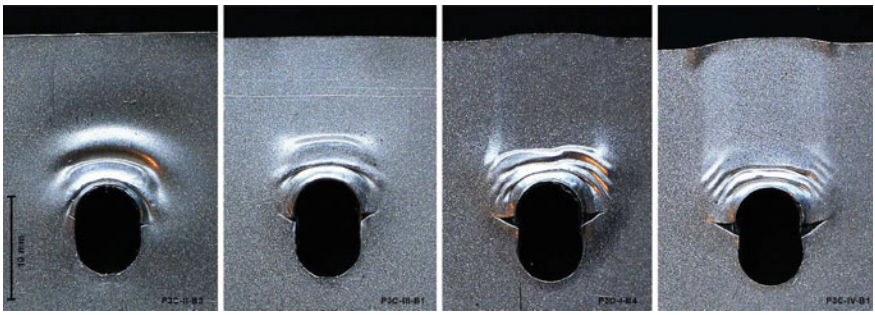

Fig. 6.7 Typical combinations of buckling and bearing failure and net-section onset cracking in laterally constrained stainless steel–CFRP laminates [10]

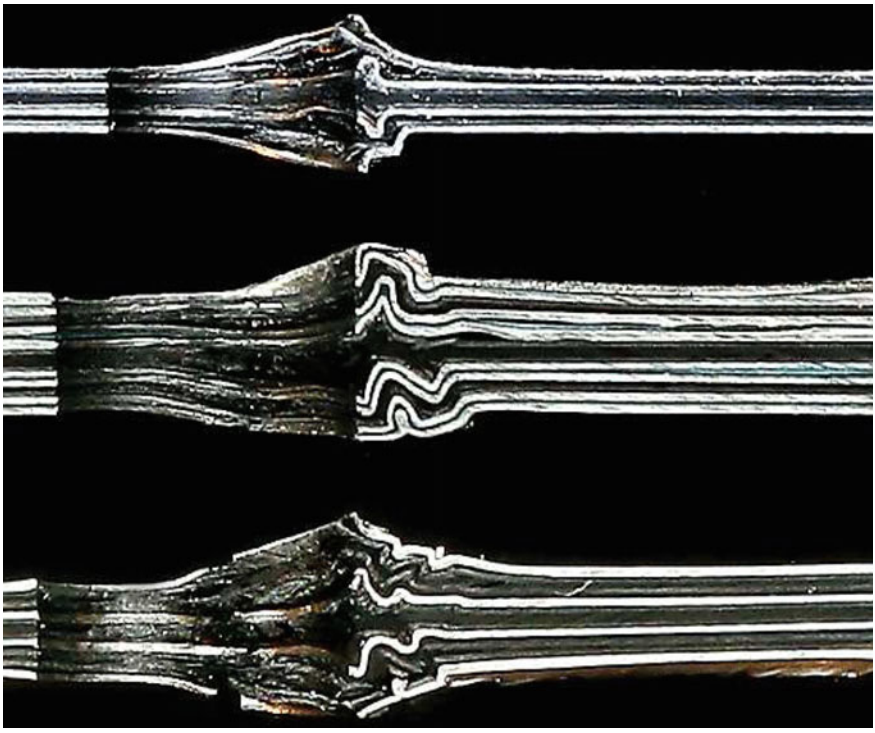

Fig. 6.8 Typical out-of-plane deformations as illustrated in Fig. 6.3 in stainless steel–CFRP laminates with 0.1 mm thin steel sheets [10]

Yamada et al. [12] for FMLs using thin titanium sheets together with carbon fibre epoxy layers.

A significant increase in bearing strength values could be obtained by improving the stability of the individual stainless steel sheets by increasing the thickness. However, Buczynski illustrated that even bonding two 0.1 mm sheets together may not be sufficient to increase the buckling stability, as the flexibility of the adhesive would not sufficiently support the individual plies, see the centre specimen in Fig. 6.8.

6.4 Diameter-to-Thickness Ratio

Hakker [5, 6] studied the bearing strength of unidirectional GLARE laminates. Aside from the edge distance-to-diameter (e/D) and diameter-to-width (D/W) ratio, he investigated the effect of diameter-to-thickness (D/t) ratio. The results of his experiments are plotted in Fig. 6.9. These data have been presented before by Wu et al. in [13].

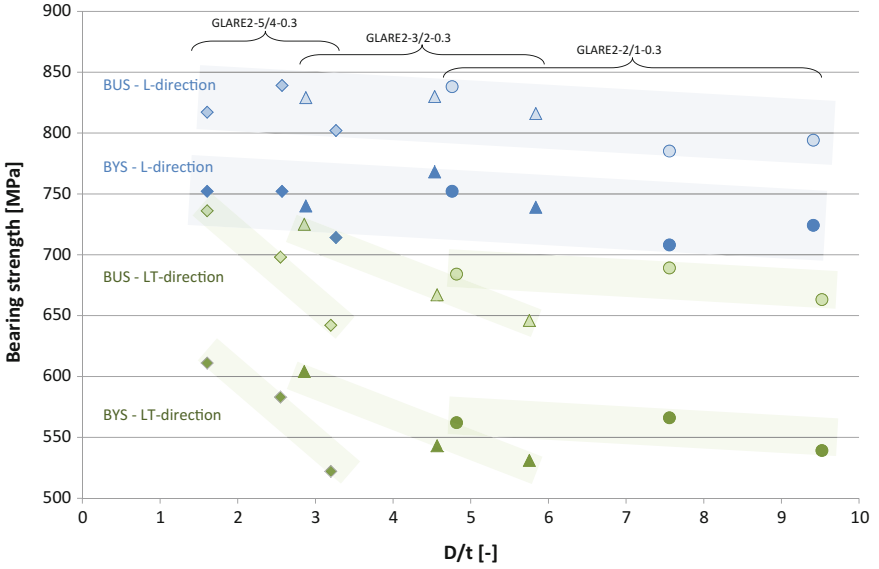

Fig. 6.9 Relation between the bearing strength and the diameter t thickness ratio D/t, data from [6]. Three diameters were tested: 4, 6.35 and 8 mm

Although Hakker concluded that there is not a clear or significant effect of increasing the D/t ratio on the bearing yield and BUS, a slight trend still can be observed. Figure 6.9 illustrates that increasing the D/t ratio decreases the bearing strength slightly. This trend should be attributed to the effect of the pin diameter itself, as was also pointed out by Hakker. Increasing the pin diameter decreases the bearing strength, which implies that the largest pin diameter of 8 mm, most commonly applied, yields the lowest strength. In any case, the results presented by Collings [14] seem to suggest that with sufficient lateral constraint, the effect of D/t will disappear.

6.5 Influence of the Diameter-to-Width Ratio

The diameter-to-width ratio (D/W), or W/D ratio, of the specimens used to establish the bearing strength influences the failure mode. As mentioned before, too low values of W/D will induce net-section failure, which may result in lower strength values. This aspect was evaluated by among others Meola et al. [15] who tested a modified GLARE laminate at several diameter-to-width ratios.

A key observation is that for values of W/D above 2, the measured bearing strength remained constant (Fig. 6.10). This implies that in order to ensure bearing type of failure mode, a width of twice the diameter should be sufficient. Comparing this value with glass fibre reinforced polymer laminates [16], this value is very low [15].

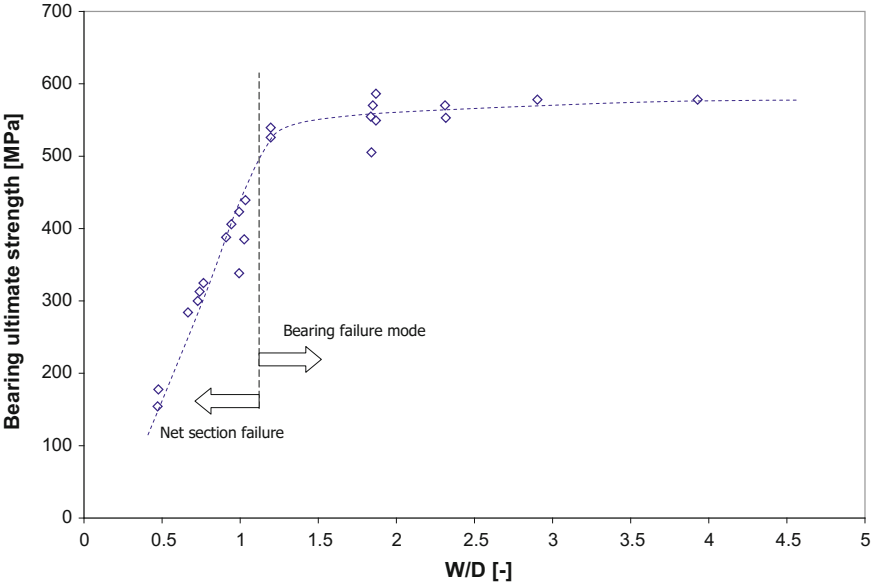

Fig. 6.10 Relation between measured bearing strength and diameter-to-width ratio (data from [15])

6.6 Influence of Edge Distance

The edge distance-to-diameter ratio (e/D) may also influence which failure mode occurs [17]. Hence, the static strength evaluation of mechanically fastened joints should consider the influence of the edge distance. Where in monolithic aluminium, the edge distance of, for example, $e/D = 2$ may be sufficient to obtain bearing type of failure, selection of the edge distance in FMLs may require some further elaboration.

To investigate the influence of edge distances on the bearing strength and failure modes, Wu and Slagter [18], Broest [19] and Meola et al. [15] performed bearing strength tests at different values for the edge distance.

The results for unidirectional GLARE2B and cross-ply GLARE3 and GLARE4B are consistent between the experiments performed by Wu and Slagter and the ones reported by Broest. It is therefore interesting to observe the difference between the standardized GLARE laminates reported by these authors and the modified lay-up tested by Meola et al., both illustrated in Fig. 6.11. Apparently, the edge distance required to obtain pure bearing strength failures with corresponding bearing strength values is lower for the modified lay-up compared to the standardized laminates reported by Wu, Slagter and Broest, as illustrated in Fig. 6.12. The transition takes place near $e/D \sim 1$ instead of $e/D \sim 2.5$.

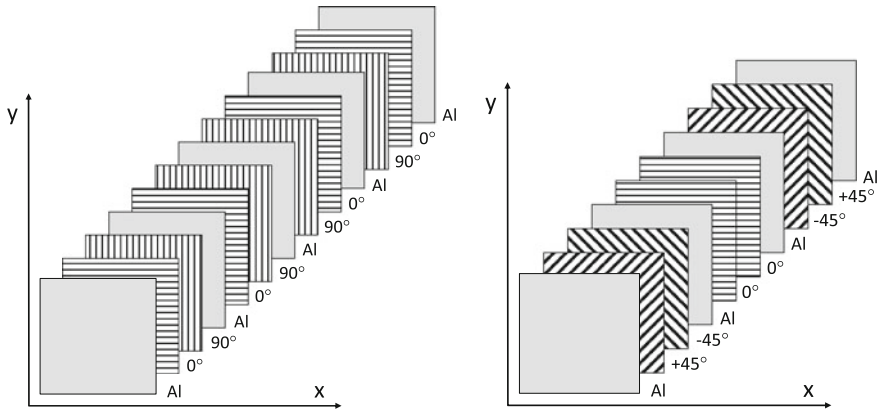

Fig. 6.11 Illustration of the GLARE3-5/4-0.3 lay-up tested by Broest [19], and the lay-up of the improved GLARE laminate tested by Meola et al. [15]

In other words, one may be able to adapt the minimum edge distance in design by changing the lay-up of the laminate, rather than changing any of the constituent materials.

6.7 In-Axis Versus Off-Axis Loading

The directionality of loading is an important parameter for design. Mechanically fastened joints, for which the bearing strength forms an important parameter, may not be perfectly loaded in their major material axes. This has led to testing FML lap joints in a uniaxial test set-up where the joint was placed under an angle, as reported by De Rijck [20].

To evaluate the influence of the load orientation with respect to the major material axes, bearing strength tests have been reported by Broest and Nijhuis [21] at loading angles of 0°, 45° and 90°. The tests were performed on unidirectional GLARE2B laminates and cross-ply GLARE3 and GLARE4B laminates.

Due to the presence of metal layers in FMLs, the influence of the fibre layers on the bearing strength remains limited, though not negligible. The results by Broest [19] and Broest and Nijhuis [21] show that unidirectional FMLs have a lower ultimate bearing strength compared to their cross-plied counterparts. The fibre layers in unidirectional FMLs only contribute with the adhesive's resistance to shear deformation, whereas in cross-ply laminates, the combination with transverse layers improves the resistance. This is schematically illustrated in Fig. 6.13.

Obviously, this resistance to shear deformation can be further improved by adding fibre layers under ±45° angles, as demonstrated by Meola et al. with their improved lay-up [15]. This improvement seems to outperform the improvements that potentially can be obtained by adding thin high-strength metal inserts at the edges as investigated by Van Rooijen [22].

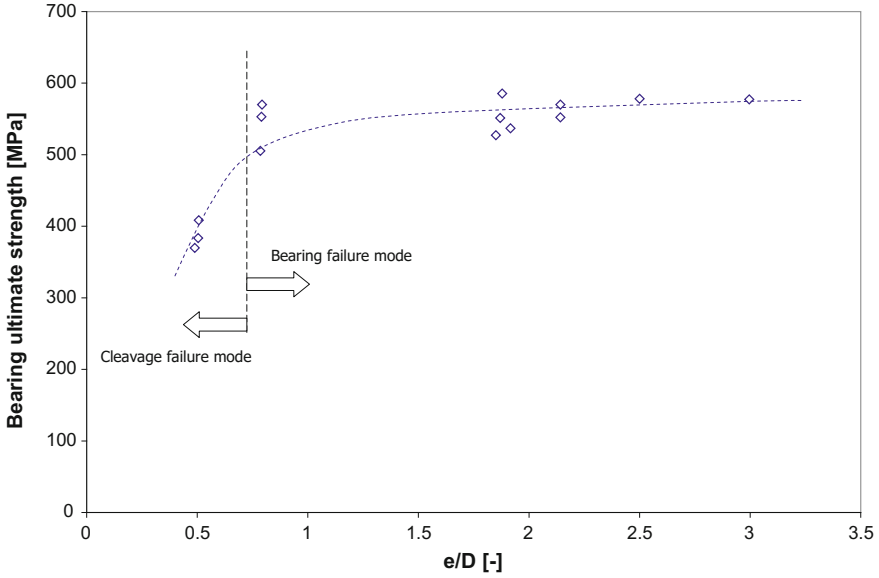

Fig. 6.12 Relation between measured bearing ultimate strength and edge distance-to-diameter ratio for laterally unconstrained bearing tests (data from [15]). A similar transition was reported by Broest [19] at $e/D \sim 2.5$)

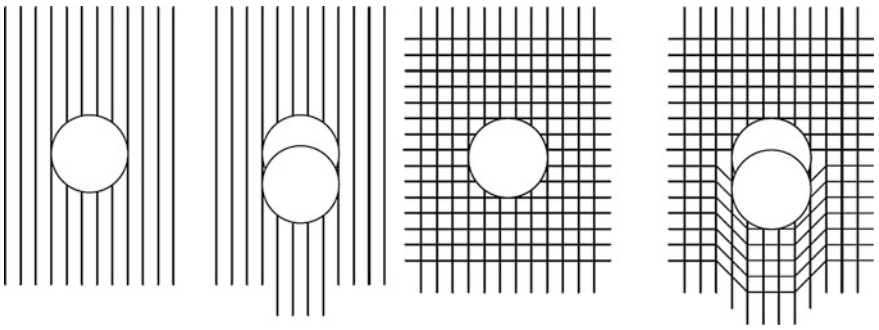

Fig. 6.13 Illustration of the influence of fibre orientation in unidirectional and cross-ply FMLs under bearing loading [19]

An interesting observation reported by Broest and Nijhuis [21] is that the dependence of the measured bearing strength on the so-called off-axis angle is fairly small, even for the unidirectional FML GLARE2A. Hence, they conclude that performing bearing strength tests under off-axis angles for determining design allowables seems irrelevant. This observation and conclusion are supported by the numerical analysis of Van Rooijen [22] who investigated the off-axis bearing

properties of unidirectional GLARE2 and cross-ply GLARE3. A comparison between the numerical results of Van Rooijen with the experimental results obtained by Broest and Nijhuis is given for both laminate types in Figs. 6.14 and 6.15.

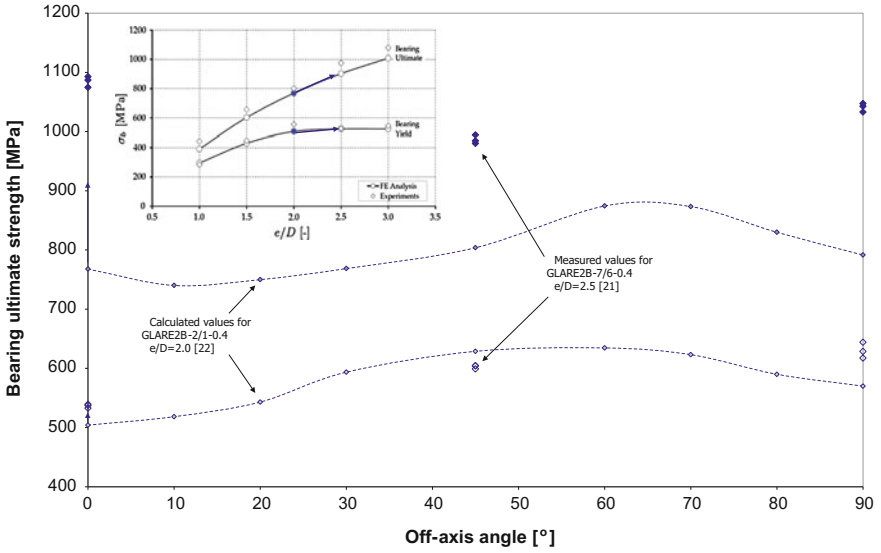

Fig. 6.14 Relation between measured [21] and calculated [22] bearing ultimate strength and applied off-axis angle for GLARE2B (insert from [22] to indicate correlation between *e*/*D* ratios)

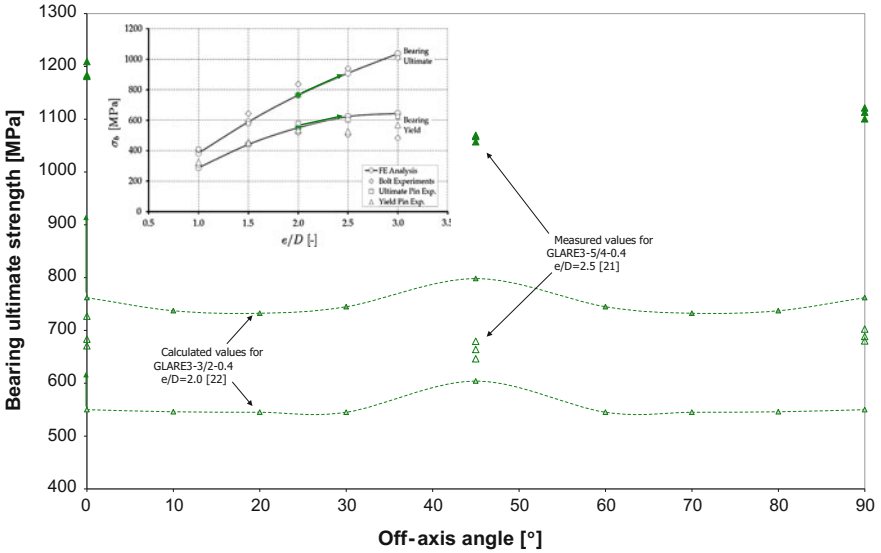

Fig. 6.15 Relation between measured [21] and calculated [22] bearing ultimate strength and applied off-axis angle for GLARE3 (insert from [22] to indicate correlation between *e*/*D* ratios)

6.8 Analysis and Prediction Methods

To evaluate the bearing strength of FMLs, various analysis methods have been proposed and reported in the literature. These methods vary from simplified analytical models to three-dimensional finite element analyses (FEA). This section provides a brief description of the most important methods for describing the bearing strength of FMLs.

6.8.1 Bilinear Constituent Representation with Rules of Mixtures

The load–deflection curve typical for FMLs can be approximated with a bilinear curve, as proposed by Slagter [4] and later again confirmed by Holleman [23] and Krimbalis et al. [24]. Slagter developed a simplified method for predicting the bearing yield and BUS. The assumption is that if the bearing strength tests were conducted on the metallic and fibre layers separately (with ASTM D953-54 for the fibre layers), one would obtain two hypothetical curves as illustrated in Fig. 6.16. In this representation, K_m and K_f represent the slopes of the linear elastic part of the load deflection curve, referred to as the elastic foundation modulus.

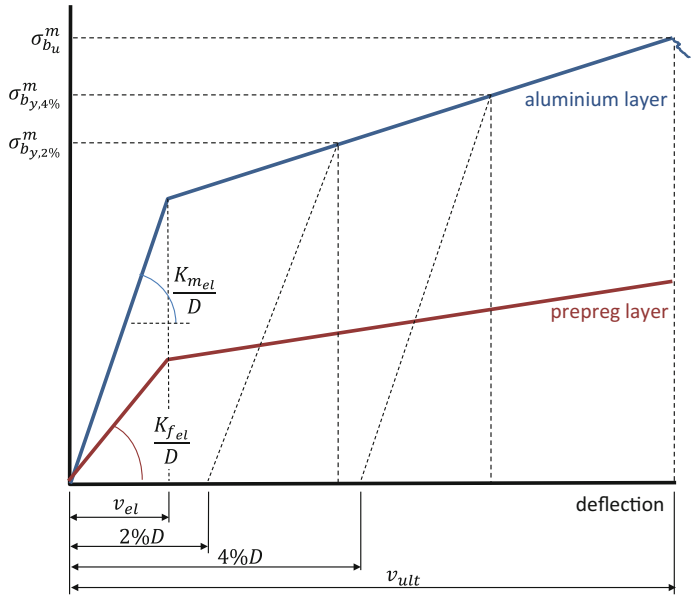

Fig. 6.16 Schematic pin-loading stress–deflection behaviour of the metal and fibre layer of an FML [4, 23]

Slagter evaluated the elastic foundation modulus K for a monolithic aluminium plate with a pin-loaded hole by making an energy analysis for the displacement of the pin in the hole. He assumed the pin to be a circular cylindrical beam resting on an elastic foundation without friction and clearance. The rigidity of the pin assured that the foundation modulus only depended on the stiffness of the foundation and not on the bending stiffness of the pin. Slagter assumed for all considered foundations an isotropic material with Young's modulus E and a constant Poisson's ratio v.

The elastic foundation modulus was calculated with

$$K = \frac{P}{v \cdot t} \tag{6.1}$$

where t is the nominal sheet thickness, and v is the deflection of the pin under the application of bearing load P [23]. Dimensional analysis reveals that the elastic foundation modulus K is proportional to the Young's modulus E with

$$K = E \cdot f\left(\frac{e}{W}, \frac{e}{D}\right) \tag{6.2}$$

which explains the name 'foundation modulus'.

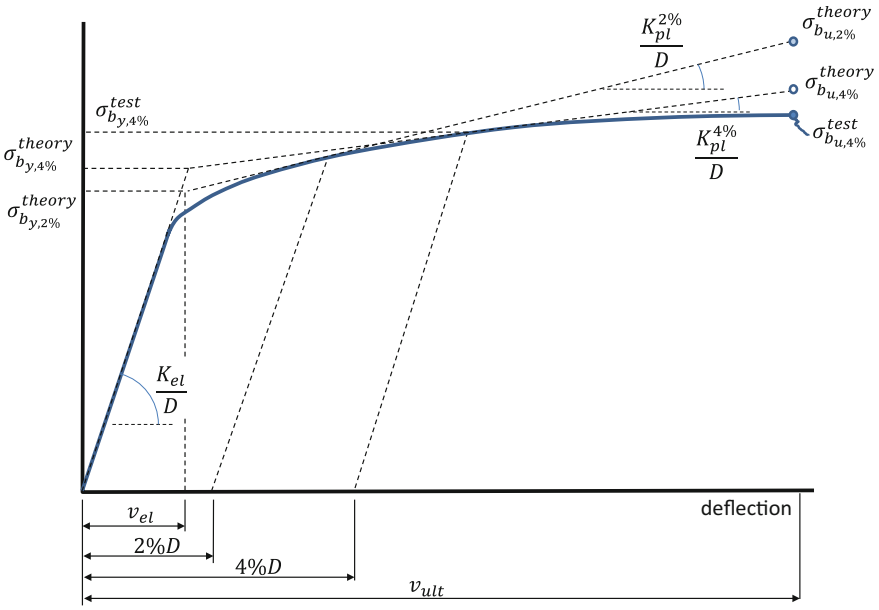

Fig. 6.17 Illustration of the idealized bilinear bearing stress–deflection behaviour in consideration of both the 2 and 4% yield point [23]

According to Slagter, bearing yield and BUS of FMLs can then be predicted with the two curves in Fig. 6.16 using the MVF approach. To enable a straightforward calculation using the MVF approach, Slagter had to assume

- that yielding of the fibre layer under the pin loading occurs at the same deflection as that of the metallic layer (v_{el} in Fig. 6.16)
- that both bearing yield and BUS of the FML correspond to the same deflections at which the metal layers reach their bearing yield and BUS.

The BYS and BUS of the FML (Fig. 6.17) are then determined with, respectively,

$$\sigma_{b_y}^{\text{lam}} = \begin{cases} \sigma_{b_{y,2\%}}^{m} \cdot \text{MVF} + \frac{K_{f,el}}{K_{m,el}} \left[\sigma_{b_{y,2\%}}^{m} + \frac{2K_{m,el}\left(\kappa_m^{2\%} - \kappa_f^{2\%}\right)}{100\left(\kappa_m^{2\%} - 1\right)} \right] (1 - \text{MVF}) \\ \sigma_{b_{y,4\%}}^{m} \cdot \text{MVF} + \frac{K_{f,el}}{K_{m,el}} \left[\sigma_{b_{y,4\%}}^{m} + \frac{4K_{m,el}\left(\kappa_m^{4\%} - \kappa_f^{4\%}\right)}{100\left(\kappa_m^{4\%} - 1\right)} \right] (1 - \text{MVF}) \end{cases}$$

$$\sigma_{b_u}^{\text{lam}} = \begin{cases} \sigma_{b_u}^{m} \cdot \text{MVF} + \frac{K_{f,el}}{K_{m,el}} \left[\left(\sigma_{b_u}^{m} - \sigma_{b_{y,2\%}}^{m} \right) \frac{\kappa_f^{2\%}}{\kappa_m^{2\%}} + \sigma_{b_{y,2\%}}^{m} + \frac{2K_{m,el}\left(\kappa_m^{2\%} - \kappa_f^{2\%}\right)}{100\left(\kappa_m^{2\%} - 1\right)} \right] (1 - \text{MVF}) \\ \sigma_{b_u}^{m} \cdot \text{MVF} + \frac{K_f}{K_m} \left[\left(\sigma_{b_u}^{m} - \sigma_{b_{y,4\%}}^{m} \right) \frac{\kappa_f^{4\%}}{\kappa_m^{4\%}} + \sigma_{b_{y,4\%}}^{m} + \frac{4K_{m,el}\left(\kappa_m^{4\%} - \kappa_f^{4\%}\right)}{100\left(\kappa_m^{4\%} - 1\right)} \right] (1 - \text{MVF}) \end{cases} \tag{6.3}$$

in which

$$\kappa_m^{2\%} = \frac{K_{m,pl}^{2\%}}{K_{m,el}}; \quad \kappa_m^{4\%} = \frac{K_{m,pl}^{4\%}}{K_{m,el}}; \quad \kappa_f^{2\%} = \frac{K_{f,pl}^{2\%}}{K_{f,el}}; \quad \kappa_f^{4\%} = \frac{K_{f,pl}^{4\%}}{K_{f,el}} \tag{6.4}$$

and $\sigma_{b_{y,2\%}}^{m}$, $\sigma_{b_{y,4\%}}^{m}$ and $\sigma_{b_u}^{m}$, respectively, the bearing yield at 2 and 4% deflection and BUS of the metal layers, often available in handbooks or provided by metal producers. In these equations, K_m, K_f, κ_m and κ_f must be determined with experiments, in particular for highly orthotropic prepreg layers [4].

According to Slagter [4], experiments support that for GLARE grades, one can assume E_f/E_m to approximate $K_{f,el}/K_{m,el}$, and that for cross-ply FML grades (GLARE3) $\kappa_m = \kappa_f$, and that the unidirectional prepreg behaves in bearing as elastic-perfectly plastic, or $\kappa_f = 0$.

Predictions with Eq. (6.1) provide excellent results for both bearing yield and BUS as illustrated in Table 6.2. All experimental results lie within 10% of the model predictions, except for the cross-ply GLARE4 laminate, of which the fibre layer contribution should be expected to lie in-between the unidirectional GLARE2 and cross-ply GLARE3 laminates. However, one has to keep in mind that the values of the bearing strength in Table 6.2 are obtained for an edge distance of $e/D = 2.0$, see also Fig. 6.18. Holleman [23] and Mattousch [25] presented significantly higher values for edge distances of $e/D = 3.0$ for some of the laminates in

Table 6.2 Comparison between bearing yield and ultimate strength obtained by bolt-type bearing test at $e/D = 2.0$ and the analytical model from [4]

Grade and lay-up	MVF	BYS			BUS		
		Test[a] (MPa)	Theory[b] (MPa)	Error (%)	Test[a] (MPa)	Theory[b] (MPa)	Error (%)
GLARE2-3/2-0.3	0.64	530	530	0.0	709	742	4.7
GLARE3-2/1-0.2	0.62		495		810	754	−6.9
GLARE3-2/1-0.3	0.71		526		856	802	−6.3
GLARE3-3/2-0.2	0.55		470		702	717	2.1
GLARE3-3/2-0.3	0.64	546	504	−7.7	789	769	−2.6
GLARE3-4/3-0.4	0.68		517		778	789	1.4
GLARE3-4/3-0.5	0.73		534		832	814	−2.2
GLARE3-5/4-0.4	0.67		513		769	781	1.6
GLARE4-3/2-0.3	0.55	518	498	−3.8	658	760	15.5

[a]Bolt-type bearing test values determined in accordance with ASTM D953-54
[b]Equation (6.1) with $\kappa_m = \kappa_f = 0.1$ (cross-ply) or $\kappa_m = 0.1$, $\kappa_f = 0$ (unidirectional), $K_f/K_m = E_f/E_m$, and $\sigma^m_{b_y} = 629$ MPa and $\sigma^m_{b_u} = 959$ MPa

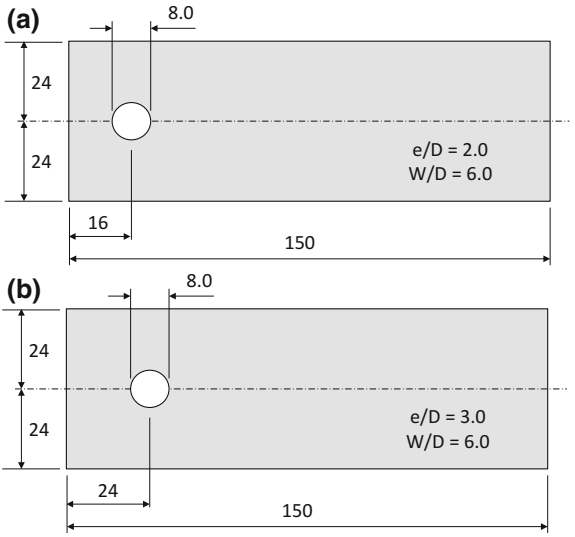

Fig. 6.18 Illustration of the dimensions of the specimens tested by Slagter [3, 4] (**a**) and the dimensions for the specimens tested by Holleman [23] and Mattousch [25] (**b**)

See Tables 6.2 and Table 6.3. Predicting the theoretical values with Eq. (6.3) then requires the bearing yield and ultimate strength for the metal layers at the same edge distance, which are given by Mattousch [25], see Table 6.4.

Table 6.3 Comparison between bearing yield and ultimate strength obtained by bolt-type bearing test at e/D = 3.0 [23, 25] and the analytical model from [4, 23]

Grade and lay-up	MVF	Test[a]			Theory ($\kappa_{a1} \neq \kappa_f$)[b]				Theory ($\kappa_{a1} = \kappa_f$)		
		$\sigma^m_{b_{y,2\%}}$ (MPa)	$\sigma^m_{b_{y,4\%}}$ (MPa)	$\sigma^m_{b_u}$ (MPa)	$\sigma^m_{b_{y,2\%}}$ (MPa)	$\sigma^m_{b_{y,4\%}}$ (MPa)	$\sigma^m_{b_{u,2\%}}$ (MPa)	$\sigma^m_{b_{u,4\%}}$ (MPa)	$\sigma^m_{b_{y,2\%}}$ (MPa)	$\sigma^m_{b_{y,4\%}}$ (MPa)	$\sigma^m_{b_u}$ (MPa)
GLARE2-2/1-0.3 L	0.70	724		1011	571	657	915	919	623	730	1073
GLARE2-2/1-0.3 LT	0.70	539		1008	493	575	837	837	502	588	864
GLARE2-3/2-0.3 L	0.64	739		991	549	629	863	868	613	717	1055
GLARE2-3/2-0.3 LT	0.64	531		976	455	530	769	769	466	546	802
GLARE3-3/2-0.3 L	0.64	657		1004	564	627	1003	918	539	632	928
GLARE4-2/1-0.4 L	0.68	667	763	1020	582	664	1009	970	576	675	992
GLARE4-3/2-0.3 L	0.55	627	719	896	543	612	946	890	535	627	922
GLARE4-3/2-0.4 L	0.62	671	759	983	563	639	978	931	535	627	922
GLARE4-5/4-0.3 L	0.50	617	710	903	530	594	924	863	521	611	898
GLARE4-5/4-0.4 L	0.57	653	759	945	550	622	957	905	535	627	922

[a]Bolt-type bearing test values determined in accordance with ASTM D953-87

[b]Bilinear representation based on empirical bearing strain hardening ratios from [23]

Table 6.4 Comparison between measured prepreg bearing yield and ultimate strength obtained by bolt-type bearing test at e/D = 3.0 [23, 25] and the values used in the MVF method [26]

Material/lay-up	t (mm)	Experiments[a]			MVF method	
		$\sigma^m_{b_{y,2\%}}$ (MPa)	$\sigma^m_{b_{y,4\%}}$ (MPa)	$\sigma^m_{b_u}$ (MPa)	$\sigma^m_{b_{y,2\%}}$ (MPa)	$\sigma^m_{b_u}$ (MPa)
[0]6	0.85	b	b	160	794	585
[0]12	1.77	b	b	159		
[90]6	0.85	b	b	82	231	565
[90]12	1.77	b	b	81		
[0/90/90/0]	0.58	171	207	373	657	689
[0/90/90/0]3	1.8	175	225	446		
[0/90]3	0.88	183	216	301		
[90/0/0/90]	0.59	152	191	373		
[90/0/0/90]3	1.78	199	237	433		
[0/90/0]	0.45	181	202	389	583	608
[0/90/0]2	0.88	212	255	469		
[0/90/0]4	1.75	196	233	427		
[90/0/90]	0.44	183	208	391	434	689
[90/0/90]2	0.89	187	230	532		
[90/0/90]4	1.76	211	244	420		
2 × 0.28 Al	0.56	689	804	1078	693	1200
Monolith Al	0.66	688	804	1194		
Monolith Al	1.3	640		1200		
Monolith Al	1.6	639	754	1200		

[a]Bolt-type bearing test values determined in accordance with ASTM D953-87
[b]Elastic until failure

6.8.2 Simplified MVF Method

The bearing strength prediction method represented by Eq. (6.3) relates both laminate bearing yield and bearing ultimate to the contribution of the bearing strength of the metal constituent and the volume fraction of the metal layers in the total laminate thickness. This is visible in Eq. (6.3) with the MVF and the (1-MVF), of which the latter is the fibre volume fraction.

To reduce the complexity of the method, Eq. (6.3) can be simplified to the rule of mixtures, discussed before for the static properties in Sect. 4.11.1 and for the blunt not strength in Sect. 5.8.1. Similar to Eq. (5.24), one could rewrite Eq. (6.3) into the form

$$\begin{aligned} S^{\text{lam}}_{b_y} &= \text{MVF} \cdot S^m_{b_y} + (1 - \text{MVF}) S^f_{b_y} \\ S^{\text{lam}}_{b_u} &= \text{MVF} \cdot S^m_{b_u} + (1 - \text{MVF}) S^f_{b_u} \end{aligned} \tag{6.5}$$

This rule of mixtures has been studied by Roebroeks [26], who developed the MVF approach for bearing strength at an edge distance of $e/D = 3.0$. The bearing yield, defined by the $2\%D$ deflection (see definition in Fig. 6.16), and the BUS were calculated with the linear interpolation rule. For this calculation, the bearing yield and BUS for the metal layers were obtained with a bearing strength test on monolithic aluminium with an edge distance of $e/D = 3.0$. These results were reported by Mattousch [25], which were, respectively, $\sigma^m_{b_y} = 640$ MPa and $\sigma^m_{b_u} = 1200$ MPa, though Roebroeks [26] used for the BYS $\sigma^m_{b_y} = 693$ MPa instead, see Table 6.4. Note that these values are higher than the values given in Table 6.2, because the edge distance here is $e/D = 3.0$ instead of the $e/D = 2.0$ in Table 6.2.

Obviously, reducing the complexity by reducing Eqs. (6.3) and (6.4) to Eq. (6.5) requires empirical assessment of the fibre layer contribution. In the attempt to evaluate the elastic and plastic foundation moduli and the κ ratios of Eq. (6.4) for the standardized GLARE grades, Holleman [23] has illustrated that for any standard GLARE grade, an assessment must be made for the longitudinal and transverse direction of the stack of fibre layers between two aluminium layers. As a result, the corresponding bearing yield and ultimate strength values of the prepreg layers must be tuned in order to obtain best fits with the bearing strength test data, as, for example, presented by Slagter [4], Holleman [23] and Mattousch [25].

Here, one has to keep in mind that testing the prepreg lay-up alone may yield different values, because the failure mechanisms differ from the mechanisms of failure of the same stack within an FML lay-up. This is illustrated in Table 6.4 by comparing the bearing yield and ultimate strength values measured by Holleman [23] and Mattousch [25] with the values determined by Roebroeks [26] for the MVF method.

6.8.3 Finite Element Analyses

An approach towards describing the bearing strength behaviour alternative to the analytical formulation of Slagter [3, 4] is through the use of FEA. Various authors have proposed FEA adopting different failure criteria or methods to define bearing failure.

For example, Van Rooijen et al. [27] presented FEA using solid elements to describe the individual layers of the FML. For the metal, he assumed elastic-perfectly plastic behaviour, while for the prepreg layers, he adopted a degradation factor for various in plane properties after failure initiation criteria were met.

Krimbalis et al. [28] suggested a different approach using FEA based on a revised compression characteristic dimension, defined as the distance between the hole edge and a point in the stress profile where the compressive stress equals the yield strength of the metal layer. In the literature, this approach is also often referred to as the critical distance method. Their definition is in agreement with their

observations in slightly modified bearing strength tests they performed [29], and the observation by Caprino et al. [9] discussed above that the aluminium layers within GLARE play a dominant role in determining the true bearing strength of a joint.

Similar to Van Rooijen, Hundley et al. [8] introduced FEA incorporating a three-dimensional progressive failure constitutive model for the prepreg layers. The interlaminar properties were described using cohesive zone formulations, while with a user material subroutine, the onset of damage in the prepreg layers was evaluated at each integration point in the mesh, similar to the failure initiation criteria adopted by Van Rooijen et al. [27].

Recently, Garg et al. [30] presented FEA using a multi-scale approach incorporated into the existing GENOA software. The multi-scale approach calculates stresses and strains at the micro-scale that are derived from the lamina scale using micro-stress theory. Although this approach is often presented as a significant advancement, one may argue that this approach is scientifically not more sophisticated than the analyses of Van Rooijen et al. [27] and Hundley et al. [8]. The reported calibration exercise with data from Hagenbeek [31] transfers the macroscopic properties established with experiments to the microscopic level; these properties are then again recalculated to macroscopic levels for predictions. The reported correlations claiming accuracy in prediction therefore merely represent a verification that this calibration is performed consistently, rather than a true validation.

6.9 Additional Studies

The studies discussed in this chapter on the bearing strength of FMLs approached the problem from various perspectives, either investigating the bearing strength experimentally, or developing predictive capabilities with analytical or numerical methods. What all these studies have in common is that they consider the subject of bearing strength of FMLs as a separate property and only for laboratory-air and room temperature environments.

Only a few studies report putting the bearing strength into context with, for example, the blunt notch strength discussed in Chap. 5, or addressing the influence of environmental conditions. This section highlights two of those studies.

6.9.1 Bearing/ByPass Diagrams

The fasteners in mechanically fastened joints often transfer portions of the load, while the remainder of the load goes around the fastener. These loads are often referred to as bypass loads. In monolithic aluminium, interaction between bypass loads and bearing loads is assumed to be small, because the ductility of the alloys

effectively redistributes the stresses. This is similar to the blunt notch strength. However, in composites the bypass loads have a significant effect on the bearing strength, requiring the assessment of the so-called bearing/bypass interaction.

A first attempt to evaluate the bearing/bypass interaction for Fibre Metal Laminates was made by Ypma [32]. Ypma tested a number of specimens, varying the number of fasteners over which the load is transferred. The approach is not according to the procedure prescribed in [33], but Ypma explains that the incentive for the exploratory study was to identify whether the interaction could be demonstrated with a simple test specimen and test set-up.

Some of the specimen configurations Ypma tested are illustrated in Fig. 6.19. He assumed the single fastener joint, illustrated in Fig. 6.19a, to represent the pure bearing strength case, while the joints with two or more fasteners represent various levels of bearing/bypass interaction.

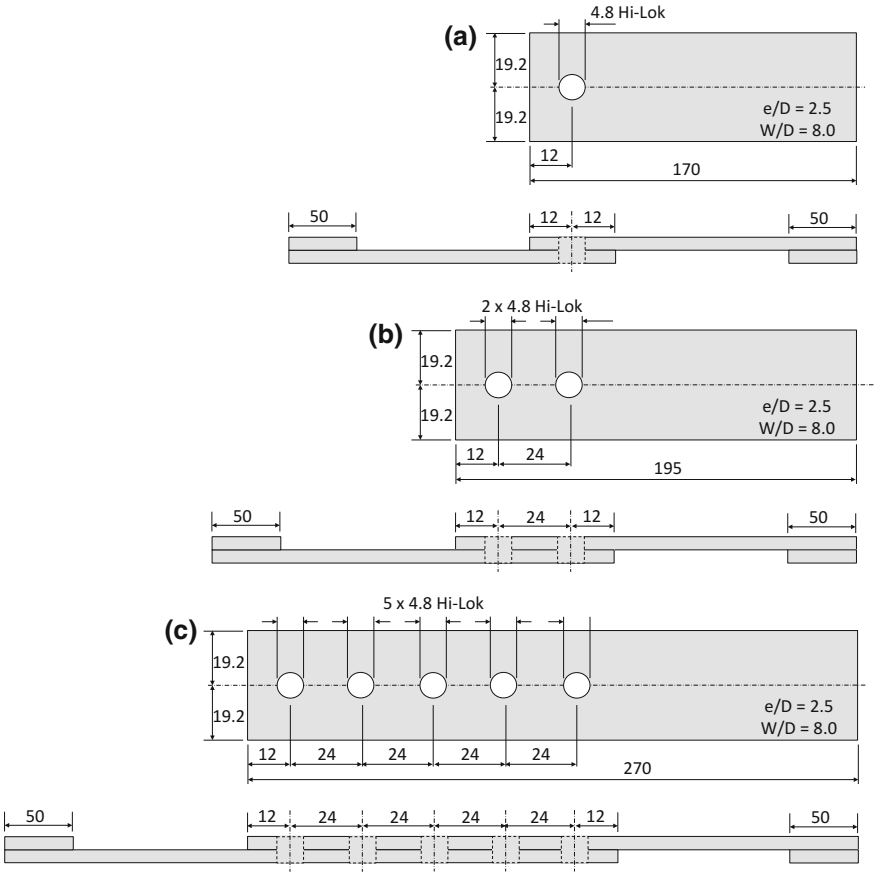

Fig. 6.19 Illustration of specimen dimensions tested by Ypma [32] with a single Hi-Lok (**a**), two Hi-Loks (**b**) and five Hi-Loks (**c**). Ypma tested in a similar fashion specimens with three and four Hi-Loks

The fastener load F_{fastener} was determined by dividing the total measured load by the number of fasteners in the specimen. Obviously, this is a crude approach, because the intermediate fasteners are known to bear less load than both outer fasteners [34]. The bearing stress was then calculated with

$$S_b = \frac{F_{\text{fastener}}}{D_{\text{Hi-Lok}} t_{\text{lam}}} \tag{6.6}$$

whereas the bypass stress was determined at the first fastener, exhibiting the highest bypass stress, with

$$S_{\text{by-pass}} = \frac{F_{\text{total}} - F_{\text{fastener}}}{W t_{\text{lam}}} \tag{6.7}$$

Because bearing/bypass diagrams are generally plotted in the form of bearing stress versus bypass strain, Ypma used the stress–strain relationships for the corresponding FML using the software developed and reported by Hagenbeek [35]. For the monolithic aluminium specimens Ypma, used the stress–strain relationships reported in [36].

Based on the experimental results, the bearing/bypass diagram was presented, which is given in Fig. 6.20. Ypma concluded that although the performed tests and the specimen geometry are far from ideal for studying bearing/bypass interaction, the experiments did demonstrate an interaction is visible for the FML GLARE. He recommended to further study this interaction using proper experiments, as, for example, proposed in [33].

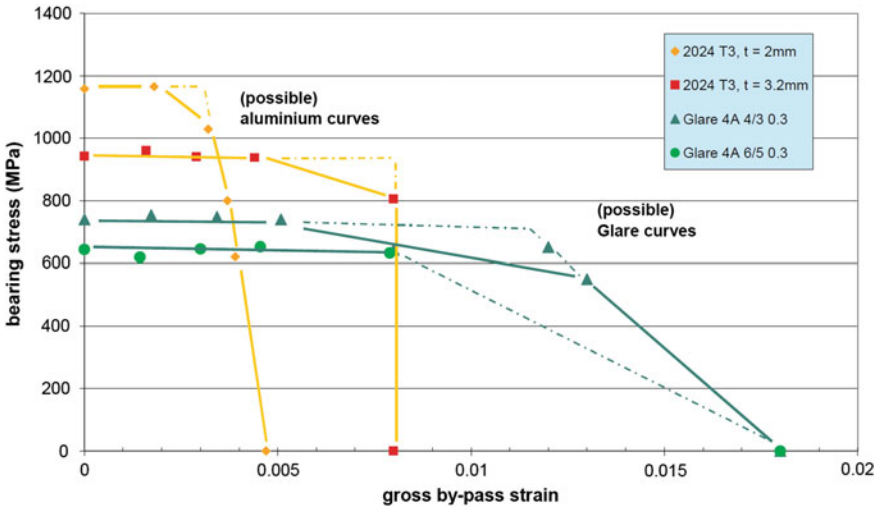

Fig. 6.20 Bearing/bypass interaction curves for aluminium 2024-T3 and GLARE4A-4/3-0.3 [32]

6.9.2 Environmental Exposure

Borgonje [37] investigated the influence of realistic hot/wet environment on the bearing strength properties, testing specimens that were exposed at a site in Australia for 2 and 6 years. He compared the observations to specimens tested without exposure at both room temperature and at 70 °C. Unexposed bearing strength tests at 70 °C were previously performed by Broest and Nijhuis [21]. In addition, specimens were tested after accelerated exposure at 70 °C and 85% RH, both for 1500 and 3000 h.

The experiments revealed that the exposure to the hot/wet environments deteriorates the BYS and BUS of GLARE. The observed reduction, however, was still less than the tests without exposure tested at 70 °C. Because the bearing strength tests were tested according to the test specification specifying clearance between specimen and its support, the obtained bearing strength values appeared to be unrealistically low. The results did seem to correlate with the bearing strength tests with and without accelerated exposure performed within the material qualification programme [38], but as Ypma already reported in [39], these were tested at an edge distance of $e/D = 2$, while Broest and Nijhuis used $e/D = 3$. For that reason, Borgonje recommended to further study the environmental influences, but to harmonize the specimen geometry and test specification, preferably using the bolt-bearing test specification.

References

1. ASTM Standard E238-84, Standard method of test for bearing strength of metallic materials, Annual Book of ASTM Standards. American Society for Testing and Materials, Philadelphia, USA
2. ASTM Standard D953-54, Standard test method for bearing strength of plastics, Annual Book of ASTM Standards. American Society for Testing and Materials, Philadelphia, USA
3. Slagter WJ (1992) On the Bearing Strength of Fibre Metal Laminates. J Compos Mater 26:2542–2566
4. Slagter WJ (1994) Static strength of riveted joints in fibre metal laminates. PhD dissertation, Delft University of Technology, Delft
5. Hakker M (1992) Geometry effects on the bearing strength of GLARE laminates. Preliminary thesis, Faculty of Aerospace Engineering, Delft University of Technology
6. Hakker M (1993) Bearing strength of GLARE laminates. Master's thesis, Faculty of Aerospace Engineering, Delft University of Technology
7. Brügemann V (2003) Test procedures for fibre metal laminates, Report TD-R-03-005. Fibre Metal Laminates Centre of Competence, Delft, The Netherlands
8. Hundley JM, Hahn HTh, Yang J-M, Facciano AB (2010) Three-dimensional progressive failure analysis of bolted titanium-graphite fiber metal laminate joints. J Compos Mater 45 (7):751–769
9. Caprino G, Squillace A, Giorleo D, Nele L, Rossi L (2005) Pin and bolt bearing strength of fibreglass/aluminium laminates. Compos A 36:1307–1315

10. Buczynski A (2009) Development of a carbon-fiber/stainless steel laminate concept—improving the bearing characteristics of carbon-fiber composites by addition of steel strip reinforcements. MSc thesis, Delft University of Technology, Delft
11. Frizzell RM, McCarthy CT, McCarthy MA (2008) An experimental investigation into the progression of damage in pin-loaded fibre metal laminates. Compos B 39:907–925
12. Yamada T, Nakatani H, Ogihara S (2011) Evaluation of bearing damage behaviour in thin titanium films-CFRP hybrid laminate, ICCM19?
13. Wu HF, Wu LL, Slagter WJ (1994) An investigation on the bearing test procedure for fibre-reinforced aluminium laminates. J Mater Sci 29:4592–4603
14. Collings TA (1977) The strength of bolted joints in multi-directional CFRP laminates. Aeronautical Research Council, Current Papers No. 1380
15. Meola C, Squillace A, Giorleo G, Nele L (2003) Experimental characterization of an innovative GLARE® fiber reinforced metal laminate in pin bearing. J Compos Mater 37 (17):1543–1552
16. Caprino G, Giorleo G, Nele L, Squillace A (2002) Pin-bearing strength of glass mat reinforced plastics. Compos A Appl Sci Manuf 33:779–785
17. Meesters (2000) Edge distance and rivet pitch in joints, a literature survey, Report B2v-00-13. Delft University of Technology, Delft
18. Wu HF, Slagter WJ (1992) Parametric studies of bearing strength for fiber/metal laminates, SLC-report SL-019-E. Structural Laminates Company, Delft
19. Broest P (2000) The influence of the edge distance on the joint strength in GLARE laminates, Report B2v-00-67. Delft University of Technology, Delft
20. de Rijck R (2003) Residual strength prediction of XJ-advanced specimens, Report B2v-03-07. Delft University of Technology, Delft
21. Broest P, Nijhuis P (2000) Determination of bearing strength, Report B2v-00-39. Delft University of Technology, Delft
22. Rooijen RGJ (2006) Bearing strength characteristics of standard and steel reinforced GLARE, PhD dissertation. Delft University of Technology, Delft
23. Holleman E (1994) Bearing strength prediction for some GLARE grades (BE2040 subtask 5.1-a), Memorandum M-683. Delft University of Technology, Delft
24. Krimbalis PP, Poon C, Fawaz Z, Behdinan K (2007) Experimental characterization of the bearing strength of fiber metal laminates. J Compos Mater 41:3109–3131
25. Mattousch AC (1994) Bearing properties of GLARE 2-2/1-0.3, GLARE 2-3/2-0.3 and GLARE 3-3/2-0.3, Report TD-R-94-010. Structural Laminates Company
26. Roebroeks G (2000) The metal volume fraction approach, Report: TD-R-00-003. Structural Laminates Industries, Delft, The Netherlands
27. Rooijen RGJ, Sinke J, de Vries TJ, van der Zwaag S (2006) The bearing strength of fiber metal laminates. J Compos Mater 40(1):5–19
28. Krimbalis PP, Poon C, Fawaz Z, Behdinan K (2007) Prediction of bearing strength in fiber metal laminates. J Compos Mater 41(9):1137–1157
29. Krimbalis PP, Poon C, Fawaz Z, Behdinan K (2008) On the pin bearing behavior of orthotropic fiber metal laminates. J Compos Mater 42:1547–1566
30. Garg M, Falugi M, Abdi F, Abumeri G (2011) Predicting bearing strength of fiber metal laminates via progressive failure analysis. 52nd AIAA/ASME/ASCE/AHS/ASC structures, structural dynamics and materials conference 19th, 4–7 April 2011, Denver, Colorado
31. Hagenbeek M (2005) Characterisation of fibre metal laminates under thermo-mechanical loadings, PhD dissertation. Delft University of Technology, Delft
32. Ypma M (2002) Exploratory investigation on the effect of bearing/bypass interaction on the static joint strength of GLARE, Report B2v-02-05. Delft University of Technology, Delft
33. MIL HDBK—17—1E. Department of Defense U.S.A
34. Schijve J (2009) Fatigue of structures and materials. Springer Science + Business Media, B.V.
35. Hagenbeek M (2000) Estimation tool for basic Material properties, ETMP_release 2, Report B2 V-00-29. Delft University of Technology, Delft, The Netherlands
36. MIL HDBK—5H, December 1998. Department of Defense U.S.A

37. Borgonje B (2002) GLARE outdoor exposure program: bearing strength, Report B2v-02-36. Delft University of Technology, Delft
38. Hoeven W. van der, Nijhuis P (2002) Qualification testing of semi-finished flat GLARE products, NLR-CR-2002-146. NLR National Aerospace Laboratory
39. Ypma M (2000) Overview of tests concerning the influence of temperature and environmental exposure on GLARE, Report B2v-00-41. Delft University of Technology, Delft